



Parametric Design and Structural Analysis of Deployable Origami Tessellation

Nixon Wonoto¹, Daniel Baerlecken², Russell Gentry³ and Matthew Swarts⁴

¹Georgia Institute of Technology, nwonoto3@gatech.edu

²Georgia Institute of Technology, daniel.baerlecken@coa.gatech.edu

³Georgia Institute of Technology, russell.gentry@coa.gatech.edu

⁴Georgia Institute of Technology, matthew.swarts@coa.gatech.edu

ABSTRACT

This paper presents a research study on a geometry and mechanism of origami for generating a deployable tessellation structure that will be tested as a large span structural system. The research explores a combination of methods for understanding the structural limitations of deployable origamic geometry by using geometric scripting with a parametric system and finite element analysis tools. This combination of methods allows deployable origamic geometry structures to be evaluated at various scales which provides information on how to optimize the geometry for a given scenario. Analog models based on biological inspirations were initially produced for studying the origamic deployment mechanism followed by a process that translated the model into a scripting based form generation using a parametric system to propagate different permutations of the same origami family. The workflow requires interoperability between the parametric system (Grasshopper/Rhino), Excel, and finite element analysis tool (LS-DYNA). The research investigates the possibilities of extracting geometric and mechanical principles of microstructure for its application to a larger scale structure as an architectural element. A recent paper by the authors discussed the general process from biological inspiration to structural evaluation of the selected origami structure (see Baerlecken et al. [1]). This paper continues the discussion with more additional information related to geometric principles of the selected origami for the case study and the technical details on the interoperability between the parametric and the structural system.

Keywords: parametric modelling, origami, deployment, LS-DYNA, permutation, scripting, tessellation.

DOI: 10.3722/cadaps.2013.939-951

1. INTRODUCTION

This paper presents a study on generating a parametric tessellation structure for a large span structural system based on the origami model as a form-generator.

Several studies of origami and folded structures by researchers such as Robert J. Lang have demonstrated the potential of origami for its application to solve various engineering problems. The application of folding and unfolding has also been used at a conceptual level for city-planning by architects such as Peter Eisenman in his Frankfurt Rebstockpark project in 1991, in which the application is used to define spatial networks on an urban scale. A more literal application of origami appears in the Yokohama Terminal by FOA in 2002, which transforms a folded structure of corrugated cardboard into a waved steel construction of origami ceiling skin. However, the current study focuses more on understandings of the geometry and architecture of origami by analyzing the structural potential of frozen states of origami generated from different deployment states using a computational parametric modelling system.

The project reviews different types of bio-origami focusing on the mechanisms, physical properties and structural potentials of biological matters such as leaves, petals and insects' wings. The relation of physical properties to the folding and unfolding mechanisms in biological matters is initially investigated during the first phase of the research. In addition, the project also discusses the structural potential of each deployment of the biological matter such as from unfolding to folding states under self weight or other additional small loads. Following the production of the origamic analog model of the biological matter, parametric model of the bio-origami was constructed utilizing parametric system combined with scripting method. Finite element analysis tool was utilized in order to examine the structural performance of the origami geometry. The analysis observed the deflection and the force reaction of the frozen state of the deployable structure in order to understand the limitation of the structure in different scales such as from a paper scale to a building scale. The research explores the possibility of implementing the principles of microstructure based on biological analogies to a larger scale so as to discover innovative structural systems.

2. GENERAL WORKFLOW

In the first phase, the research observed analog and digital models representing the folding and unfolding mechanisms of leaves, insect wings, segments of earwigs, grasshoppers, crickets and praying mantes. The process involved investigation on several studies done by researchers such as Forbes [3] and Haas [5] in order to observe the mechanisms, physical properties and structural potentials of biological matters. Forbes [3] studied the wing folding mechanism in beetles in both rest and ready-to-fly positions by observing tension and stiffness lines of the wings. Haas [5], on the other hand, studied the wing movements of Dermaptera and Coleoptera during folding and unfolding states using angle and vector analysis. In the case of insect wings, following the approaches done by Forbes and Haas [5], the research includes the understanding of which creases are produced when the folding and unfolding mechanism occurs at any given angle while paying attention to the tension and stiffness lines when the folding occurs. In the case of leaves, following the approach done by Kobayashi et al. [8], the research includes the understanding of the level of structural compactness resulting in maximum symmetrical foldings, which depends on the existing variables of the leaf such as angles between the mid-rib and veins. The first phase envisioned that the variable of angles between the mid-rib and veins of the leaf identified by Kobayashi et al. [8] could be utilized as one of the parameter in order to define the mechanism and physical properties of the leaf structure in the parametric modelling process.

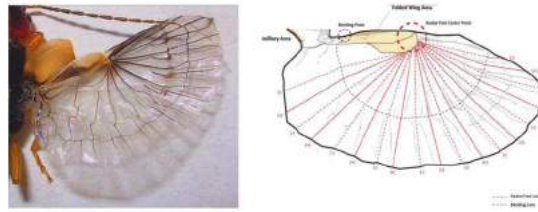


Fig. 1: Diagram of folding mechanism, earwigs.

In the second phase, analog models based on origami folds were proposed. The making of the analog models involved some basic origami operations such as mountain and valley folds, squash folds, pleats, and reverse folds. The scale of the analog model constructed varied from micro to larger paper folds in order to observe the origami deployment mechanism that resulted from the creases. It is important to note that the research focuses on studying rigid origami in which each panel is bounded by creases acting as hinges, and each panel face is not allowed to bend or stretch during each state of deployment [11]. This phase investigates the kinetic mechanism in each state of deployment of the various scales of the built rigid origami through the analog model and makes an initial approximation of the level of deformation the origami can tolerate in each state of deployment in order to understand its potential flexibility and stiffness.

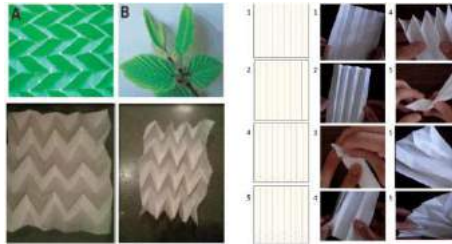


Fig. 2: Diagram of folding patterns of leaves (left top), analogue models (left bottom), processing analog model (right).

In the third phase, selected analog models of the origami were translated into a parametric system followed by a structural evaluation (LS-DYNA). This phase dealt with discovering the mathematical principle of the geometry and the mechanism of the origami. The basic principles of rigid origami such as restrictions on the face panel stretchability were embedded in the parametric model, and the principle of the folding and unfolding of origami was implemented in the system by using the trigonometric function for solving the rotation angle of the hinge. The generated model from the parametric system was then transferred to LS-DYNA for structural evaluation, which was bridged via vb.net scripts to produce syntactical interoperability. Information regarding the structure of the system like the Element ID as parts identifier, the Node ID determining element connectivities, and the Material ID were extracted from the parametric system for LS-DYNA input. One difficulty that arose during this process was related to the complexity of the data exchanged during the process. Grasshopper and Rhino operate with independent NURBS surfaces, whereas LS-DYNA operates with polygonal meshes. The details of this interoperability issue will be discussed later in this paper. After successfully exchanging the data and running the simulation, numerical feedback from LS-DYNA for nodal displacements and force reactions of the model were converted to scatter charts in Excel for further analysis on the structural potential of the model. In the last phase, prototypes were developed through digital fabrication, and the model's structural properties were further tested.

In phases 3 and 4, the understanding and selection of materials and manufacturing strategies played a pivotal role during the whole process. In the parametric system, each facet of the geometry

was assigned with a material ID (MID) in which the information of the density, the modulus of elasticity and poisson ratio of specific material were assigned to the ID in the “dyn” file as input for LS-DYNA. In this research, PETG (glycol-modified polyethylene terephthalate) was considered suitable to satisfy the conditions of the kinematic requirements and deployability of the origami structure. PETG material has high tensile strength (53.7 ± 1.9 Mpa), which allows high elongation at yield, and PETG also has high impact resistance, especially at relatively higher temperatures (114 ± 25 J/m at 25.5°C) [4]. At lower temperatures (-8.7°C), although reduced, PETG still has relatively high impact resistance (84.9 ± 9.4 J/m) [4]. High tensile strength allows PETG to have a higher plastically deformable level without fracturing, which is suitable for its application to the retractable nature of the studied origami structure. In addition, PETG is easy to mold due to its noncrystallizable characteristic, which makes its viscous flow temperature lower than 130°C [7]. Because it is easy to process and mold, PETG makes the entire fabrication process more efficient in general. The usage of PETG material for the case study will be described in more detail later in this paper.

3. ORIGAMI APPLICATION AND TYPES

The term “origami” is derived from the Japanese *oru* meaning “to fold”, and *kami* meaning “paper”. Although some of the current types of origami allow cutting paper (Kirigami), and gluing multiple folded papers together (Modular Origami), according to Durreisseix [2], the traditional origami usually uses only a square planar sheet of paper with techniques for making straight folds, without tearing, cutting or gluing. Other origami types may have embedded kinetic mechanisms within the model (Action Origami), and some may have repetitive figures similar to tiling patterns (Origami Tessellations). Interestingly, some models of origami may possess more than one of those characteristics simultaneously such as Miura-ori, which has both tiling patterns and kinetic mechanisms.

Recent applications of origami by architects and engineers are utilized to attain architectonic quality which provides form, kinetic properties and structure simultaneously. Variations of folding techniques, creasing depths, and their repetitions provide various stability to structures as well as unique mechanisms and qualities of space. The nature of origami provides structures that can be mechanically folded and unfolded without having plastic deformation or “locking” which prevents deployment [9]. The ways that origami has been widely used for form finding, design mechanisms and structural studies are strongly related to the mathematical principles of paper folding which are developed by researchers such as Jacques Justin, Humiaki Huzita and Robert J. Lang. Jacques Justin and Humiaki Huzita discovered the six axioms describing parametric equations of paper folding, which can be used as grammatical rules containing angles and lines to develop complex 2-D pattern for folding. Robert J. Lang developed software (TreeMaker) which is able to construct full crease patterns for a wide variety of origami bases.

Other than architects and engineers, the application of origami has also been used widely for other purposes such as for aerospace industries, food packaging, folding drink containers, car-airbags, spacecraft antennas and many others. Due to the variety of purposes intended by the application of origami, it is very difficult to categorize origami types. However, most of them have similar advantages related to the structure of origami such as being lightweight, structurally stable, deployable and compact. One of the origami types that has these advantages is the Miura fold which was invented by the astrophysicist Koryo Miura for large solar panel arrays for space satellites. The solar panels which provide satellites with electricity have to be compactly folded and fit into the bay of a space shuttle, for which Miura-ori, due to its compactibility when folded, is suitable. Miura-ori has one degree of freedom and can be deployed by one motion of pulling or pushing the opposite ends in order to unfold or fold the whole model.

This research selected Miura-ori for the case study. The selected Miura-ori can be categorized as rigid origami, as described earlier, whose panel is bounded by creases acting as hinges, and each panel face is not allowed to bend or stretch.

4. PERMUTATIONS AND ORIGAMI TRUSS

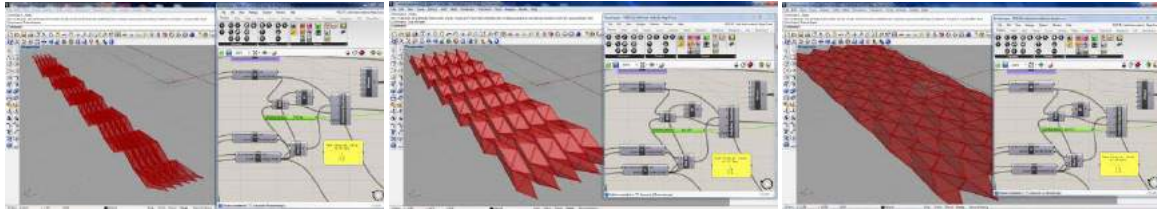


Fig. 3 : Geometric folding permutation of Miura ori (Left: Maximum Folded, Middle: In-between (50%), Right: Fully unfolded).

Fig. 3 shows different folding permutations from fully packed to fully unpacked configurations (flat 2-dimensional configuration) generated by using the parametric system (Rhino/Grasshopper). During the case study, the retractable roof could not be in a fully unpacked configuration due to its lack of structural value in the flattened mode. For the structural analysis purpose, the selected range of folding angles are ϕ equal to 43° , 58° and 71° . The geometry input for structural analysis (LS-DYNA) was generated from Grasshopper and was syntactically bridged using vb.net scripts for managing interoperability. LS-DYNA can exhibit a post-buckling response and is considered suitable for the case study due to the occurrence of large deformation in some of the generated permutations.

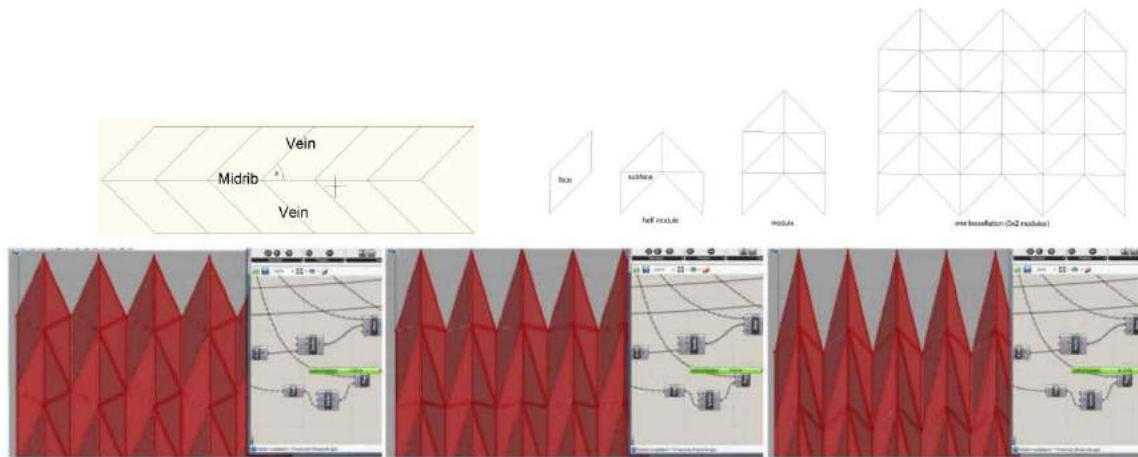


Fig. 4 : Variable of angle between mid-rib and veins (top left), and different permutation from wider angle (bottom left) to smaller angle (bottom right).

In addition to the folding angle and the number of modules in tessellation (see Fig. 4 top right for definition of a module), the angle between the mid-rib and the veins also become a part of the adjustable variable. Along with 3 different variables and materials, the permutations are organized as described below:

1. 27 permutations with Material: Edge=5mm, Face=5mm
2. 27 permutations with Material: Edge=2.5mm, Face=5mm
3. 3 permutations with Material: Edge=5mm, Face=2.5mm

The research generated 27 initial permutations (3x3x3) with the same material thickness in order to make a comparative study between each permutation with three different inputs on three variables such as the angle between the mid-rib and the vein, tessellation density and the folding angle. The comparative study observed the changing of the dimensions and the volume of the bounding box

containing the whole tessellation of each permutation of the model. The overall findings of initial comparative study reveals that given the same amount of tessellation density (number of modules) in X and Y on a defined rectangular plane and given the same folding angle as the angle between the mid-rib and the veins increase, the overall height of origami tessellation also increases when folded. The relation of the tessellation height of origami and the overall structural performance of the tessellation will be further discussed later in this paper. In addition, the overall findings also reveal that given the same case of tessellation density and folding angle, as the angle between the mid-rib and the veins increase, the overall width of origami tessellation also increases when folded. This idea suggests that the higher angle between the mid-rib and the veins takes longer time to fold and unfold compared to the lower angle. However, it allows the structure to fold more compactly. This notion was also explained by Kobayashi et al. [8].

Shift of Origami Grid [m]	Tessellation Density in X	Tessellation Density in Y	Folding Angle (Degree)	Origami Height [z] [m]	Origami Width [x] [m]	Origami Length [y] [m]	88 Area (m ²)	88 Volume (m ³)
-2.00	10.00	12.00	43.20	1.67	23.59	99.96	2358.04	3944.34
-2.00	10.00	12.00	58.38	2.08	16.84	98.96	1606.83	3461.27
-2.00	10.00	12.00	71.00	2.30	10.09	98.23	991.14	2277.03
-2.00	12.00	14.00	43.20	1.33	23.34	99.15	2333.67	3100.49
-2.00	12.00	14.00	58.38	1.88	16.79	98.30	1650.35	2775.09
-2.00	12.00	14.00	71.00	1.86	10.97	97.61	982.86	1828.72
-2.00	14.00	16.00	43.20	1.12	23.57	98.09	2324.14	2019.84
-2.00	14.00	16.00	58.38	1.40	16.90	97.87	1653.52	2307.92
-2.00	14.00	16.00	71.00	1.55	10.28	97.23	999.08	1544.68
0.00	10.00	12.00	43.20	2.02	24.19	96.69	2338.64	4726.80
0.00	10.00	12.00	58.38	2.51	17.76	95.03	1687.41	4243.49
0.00	10.00	12.00	71.00	2.79	11.21	93.92	1053.28	2940.06
0.00	14.00	16.00	43.20	1.71	23.97	95.05	2292.48	3911.05
0.00	14.00	16.00	58.38	2.12	17.37	94.02	1632.74	3461.56
0.00	14.00	16.00	71.00	2.23	10.65	92.95	980.10	2225.50
0.00	16.00	18.00	43.20	1.48	23.80	94.87	2258.12	3333.91
0.00	16.00	18.00	58.38	1.83	17.07	93.27	1592.21	2917.71
0.00	16.00	18.00	71.00	2.03	10.23	92.24	943.20	1912.39
2.00	10.00	12.00	43.20	2.25	26.83	94.10	2525.04	5688.86
2.00	10.00	12.00	58.38	2.84	22.68	91.98	2085.79	5914.30
2.00	10.00	12.00	71.00	3.20	18.52	90.33	1672.67	5360.81
2.00	12.00	14.00	43.20	1.94	27.13	92.99	2522.32	4893.85
2.00	12.00	14.00	58.38	2.44	23.26	90.88	2113.73	5138.35
2.00	12.00	14.00	71.00	2.76	19.43	89.24	1794.23	4785.49
2.00	14.00	16.00	43.20	1.71	27.18	92.03	2519.75	4351.00
2.00	14.00	16.00	58.38	2.17	23.78	89.89	2137.80	4032.13
2.00	14.00	16.00	71.00	2.43	20.27	88.26	1789.29	4378.90

Tab. 1: Initial comparative study on tessellation’s dimensions and volumes for generated 27 permutations.

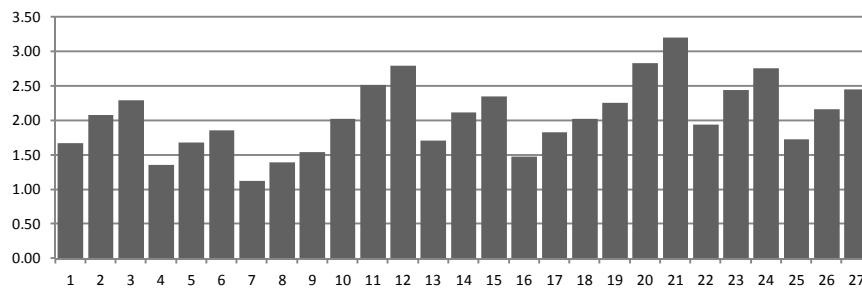


Fig. 5: Changes of the Origami height in 27 permutations.

The initial 27 permutations were then transferred to LS-DYNA to run the structural simulation. The simulation shows that in the full scale forms, for the Toyota Stadium roof, the origami requires more stiffness in the transverse direction to span the opening, while it also has to maintain its capability to smoothly deploy without any locking. The concept of an “origami truss” is introduced as a solution in order to stiffen the origami structure while still allowing smooth deployability of the retractable roof.

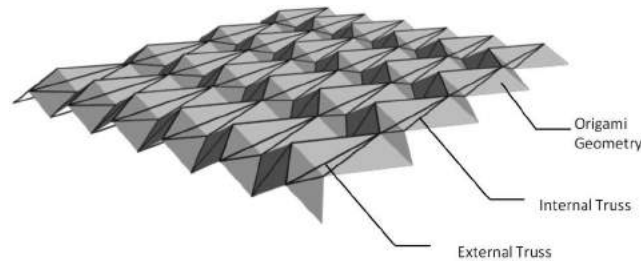


Fig. 6: Application of origami truss.

The origami truss consists of an external and an internal truss which when combined with the origami surface can be envisioned as a stiffened sail. The internal truss is positioned along the edges of the origami structure and is always stuck to the surface of the origami with the same dimension to the distance of the nodes with which it connects. The external truss is not stuck to the surface and is able to elongate and shorten. The dimension of the external truss relies on the state of the folding angle of the tessellation. When, for instance, the folding angle is extremely reduced, the tessellation will be almost flattened, and the stretch of the truss will reach the maximum. The external truss members are constructed with nested round tubes which have a locking mechanism that will lock axially once the deployed structure has reached its opened or closed position.

The other way for stiffening the origami structure in its large scale application (1:1) is by thickening the material. The first 54 (27x2) permutations of origami has a face thickness of 5mm with different edge thicknesses (5mm and 2.5 mm). These conditions envision the solution of stiffening the origami structure through surface thickening. Research on folding thickened origami was done by Hoberman [6] using the axis-shift approach that allows complete folding and unfolding, but it cannot be applied to non-symmetric vertices. Tachi [10] on the other hand, used a material tapering method in order to allow foldability, which is done by solving the dihedral angle between adjacent facets of thickened origami modules when folding to prevent the collision of volumes. The tapering method can be used for nonsymmetrical vertices allowing a more organic form, but the model cannot be fully folded to angle = 0 in order to prevent the half volume of tapered material reduced to 0. Although the approaches to stiffening proposed by Hoberman [6] and Tachi [10] propose interesting alternatives, the current origami model in this paper is intended to gain folding compactability in deployment without significant modification in the geometry such as the tapered shape, and the considered approach is also intended to allow nonsymmetrical figures to deploy.

The final 3 permutations that are generated by the parametric system envision the usage of an origami truss by thickening the edge material to 5mm and reducing the face thickness to 2.5mm. In this way, the edges of each origami module act as an internal truss, and additional external truss members are added to increase the stiffness of the whole structure. This system is considered suitable because it provides flexibility and rigidity at the same time, which is similar to the principle of the leaf having veins and ribs as structures of its membrane as described earlier in this paper.

5. GEOMETRIC PRINCIPLES OF THE MIURA-ORI PATTERN

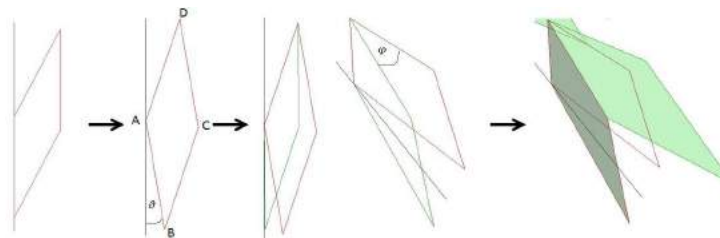


Fig. 7: Rotational principles of Miura-ori.

Miura-ori can be recognized geometrically by its glide reflection form of symmetry, in which the motif is translated and reflected not necessarily in a straight line. The original motif is reflected and flipped front to back, which makes the valley and mountain folds switch interchangeably. Miura-ori is flat foldable origami in which each module of Miura-ori satisfies the Maekawa's theorem $Mountain-Valley = \pm 2$ at a single vertex. This can be seen in a modular level where each module has either 3 mountain and 1 valley or vice versa. Following Kawasaki theorem, the number of the mountain and valley assignment at a single vertex are even such that $\beta_1 + \beta_3 = \beta_2 + \beta_4 = 180^\circ$ where $\beta = \text{angle between creases}$. Following those two theorems, each module of Miura-ori can be successfully flat foldable at single vertex. The pattern gives the origami the capability to be deployed from being completely flattened ($z=0$) to compacted with Z thickness ($x=0$).

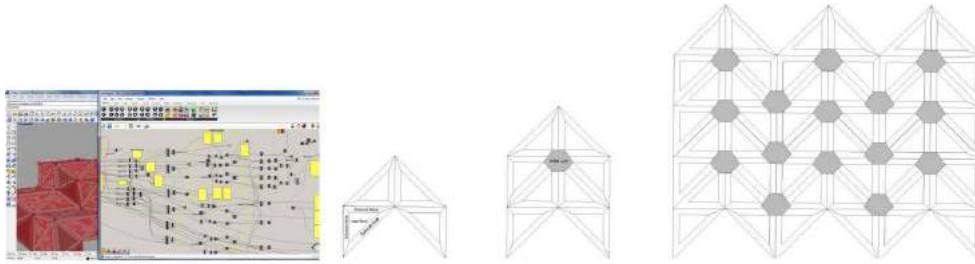


Fig. 8: Topological organization for materiality.

The pattern has one degree of freedom, and the state of its deployment is defined by one independent parameter, the angle of rotation value. In Euclidean geometry, the individual facet of the origami can be defined as a parallelogram with opposite sides having equal length, and the opposite angles having equal measure. As can be seen in the Fig.4 (top-right figure), when each of the facets has one bisecting diagonal, it produces two triangular facets in a parallelogram with the same area which is termed as subface, and when the angle between the diagonal bisecting line (adjacent side) and the Y-axis parallel fold (opposite side) of the top triangular facet is 90° (right triangle configuration), the diagonal line is parallel to the X-axis when the pattern is completely flattened. In all states of deployment, the edges that are described as the mid-rib of the origami (see Fig. 4) must remain parallel to the Y-axis. As the patterns begin to fold, the facet will be rotated in θ (XY plane), as well as rotated in φ around AD axis to take on the Z thickness (see Fig. 7 and Fig. 9). The Z thickness gives the pattern structural possibilities. Formulas (1) and (2) express the rotation equation for φ and θ . In the formula, α is the angle between the bisecting line of the parallelogram facet and the vein line of origami (see Fig.4). The capacity for the pattern to span depends on the rotation value and the flexural stiffness of the folded material at the folds.

$$\varphi = \cos^{-1}(\tan(\alpha) / \tan(\alpha + \theta)) \quad (1)$$

$$\theta = \tan^{-1}(\tan(\alpha) (1 - \cos(\varphi)) / (\tan^2(\alpha) + \cos(\varphi))) \quad (2)$$

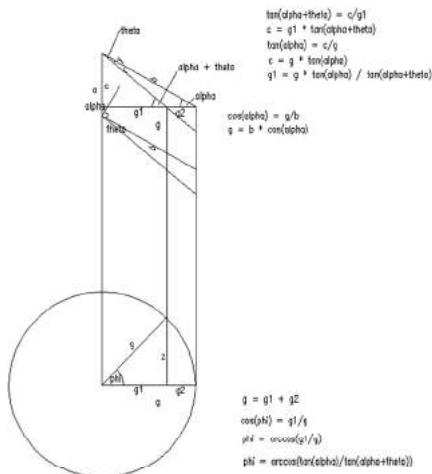


Fig. 9: Geometric derivation of Miura-ori pattern.

6. INTEROPERABILITY BETWEEN PARAMETRIC AND STRUCTURAL ANALYSIS SYSTEM

The parametric model of Miura-ori was constructed using the Grasshopper plugin to Rhino. The model was constructed from an initially defined set of points which produced a grid system used to create the facets of the origami. The distance and amount of points can be adjusted to define the scale and angle between the mid-rib and the veins of the origami as well as the number of modules for the whole tessellation system. The facets are rotated in and (see Fig.9) , and the rotated facets are mirrored to produce their symmetries to generate each module of origami.

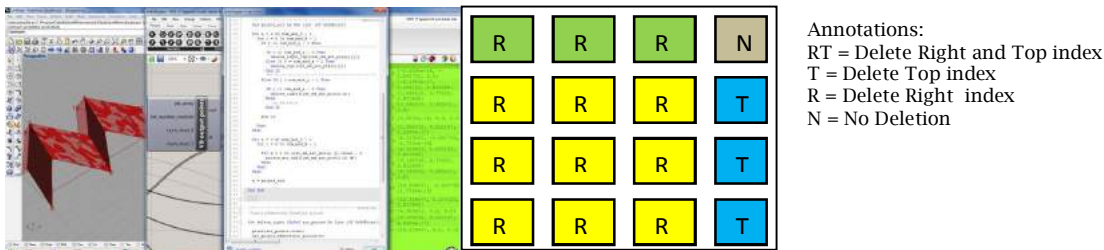
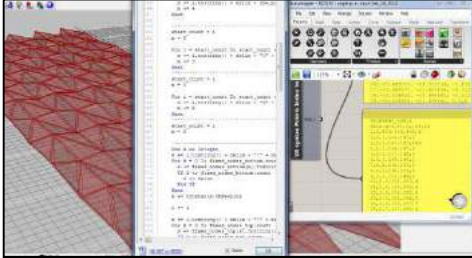


Fig. 10: Diagrams of data management within grasshopper/vb.net for polygons.

During the process, scripts were developed for converting each of the NURBS polygons generated by Grasshopper into an integrated polygonal mesh data structure for LS-Dyna. Each of the exported geometric entity was assigned with a unique ID and was topologically organized. In the parametric system, the topological data constructing the origami faces and the order of each face forming the rows of origami modules were organized utilizing script based method in which after the processing, each face will then possessed its own organized element ID as parts identifier. Each of the organized face was defined by the Node ID determining element connectivities.



Element ID	Material ID	n1	n2	n3	n4
1	2	863	143	144	1
2	3	1	144	145	2
3	2	8	145	148	808
4	2	1	146	147	2
5	2	2	147	148	3
6	3	3	148	146	1
7	2	2	149	150	3
8	3	3	150	151	5
9	2	5	151	149	2
10	2	3	152	153	4
11	2	4	153	154	5
12	3	5	154	152	3
13	2	4	155	156	5
14	3	5	156	157	7
15	2	7	157	155	4

Fig. 11: Geometric data extraction from parametric system.

The process initially required B-rep extraction of geometrical entities such as the numerical index of points and reorganized the entire index using script to produce a new combination of B-rep data structure for defining geometries that were acceptable for LS-Dyna. When constructing new elements such as the truss members, the process had to reuse the organized B-rep data structure. This made the whole process cumbersome because Grasshopper automatically generates a new nodal index when a new geometry is created. The script involved some deletion process on some overlapping points automatically generated by Grasshopper during the parametric modelling process. Two alternatives were proposed during the research project. The first option was to create a customized script that served as points' overlapping detector eliminating or joining any overlapping points in a certain close distance tolerance. In this case, the numerical input for the distance tolerance could be set as minimum as possible, which indicated the overlapping position of the points. The script might be suitable for the purpose, but the process would require longer time to compute because in this case, the script would be required to check every location of the point of the whole tessellation. The second option was to create a system that avoided any potentiality of such occurrence using predefined data management illustrated in the diagram Fig. 10. In this case, The second option was considered because it had more guarantee in order to prevent the occurrence of overlapping points, and it took less time to compute. The subsequent steps were entirely numerical manipulation in order to reorganize the nonoverlapped topological index of points to define the element connectivity. Thus, almost the entire modelling process is scripted based to manage the geometry and the topological index.

For defining materiality, the process required modifying the topological structure by adding new topological entities to each of the existing facets. The edges of each subface were offset to maintain a uniform distance between the edges of the original and new subface (see Fig. 8). The new smaller facet (cap face) was surrounded by 3 subsub faces. Each topological entity was assigned with an index of material ID representing the thickness and character of the materials (PETG or steel trusses). The organized data structure of the topological index consisting of the Element ID, Node ID and material ID were then syntactically organized with the vb.net script to produce syntactical interoperability between the parametric system (Grasshopper) with LS-Dyna.

In addition to the Element ID, Node ID and material ID as inputs for LS-Dyna necessary to run the simulation, additional scripts were made in the parametric system in order to extract the list of nodes that were located in the middle of the tessellation for tracking the Z-displacement value of the tessellation during the structural simulation. The list of nodes acting as the boundary of the tessellation (that are the points attached to the big kneel truss) were also extracted as points that were considered fixed during the simulation. All this information was generated for the structural evaluation in LS-Dyna.

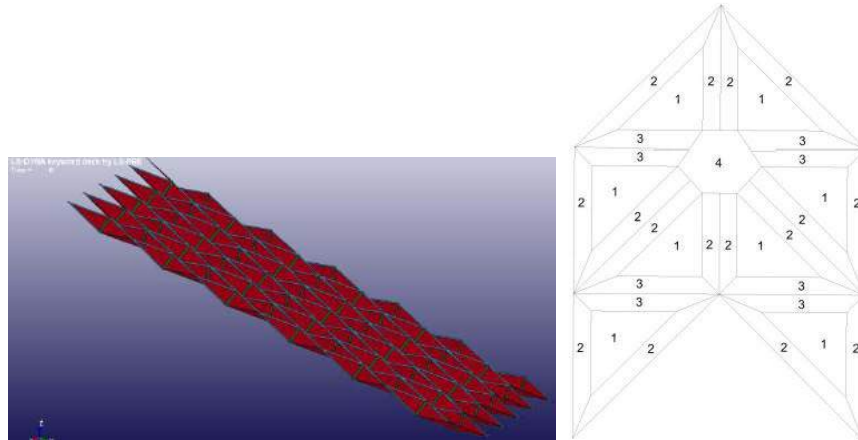


Fig. 12: Example of permutation with material ID configuration: 1 panel centre, 2 single edge, 3 double edge, 4 6-legged node.

7. STRUCTURAL EVALUATION IN LS-DYNA

The structural evaluations are based on 57 permutations generated from Rhino/Grasshopper with different inputs based on three different variables, namely the number of modules, the angle between mid-rib and vein, and the angle of deployment, as described earlier in this paper. The angle of deployment is varied at approximately 25%, 50% and 75%. The materials for the edges are varied from thinner edges representing a continuous linear hinge for deployment of the origami to thicker edges representing the installed origami truss. For this initial study, PETG material is used, which has high tensile strength that allows a higher plastically deformable level without fracturing. Such high elongation capabilities may become necessary due to the bending requirements at the edges. In addition, as previously described, at cold temperatures such as -8.7°C , PETG still has relatively high impact resistance ($84.9 \pm 9.4 \text{ J/m}$). In Aichi prefecture, the coldest weather is in January (average = 0.8°C), which means that the PETG material is still able to retain its impact resistance level even at the coldest known temperatures.

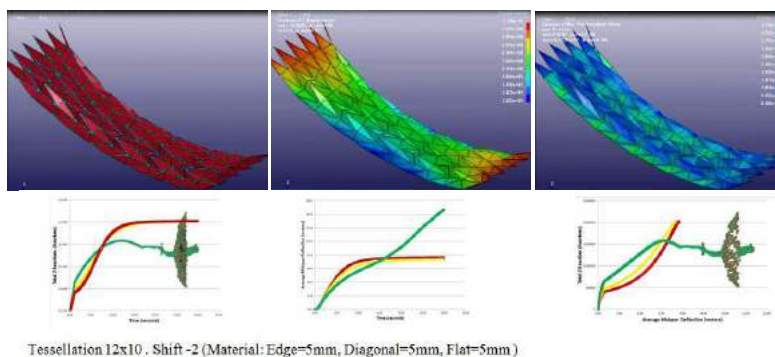


Fig. 13: Structural Analysis (LS-Dyna).

The models were evaluated for their structural potential under their own self-weight. Batch scripts were made to run multiple simulations at a time. The feedback from LS-Dyna show the numerical output of time versus the force reaction of gravity towards tessellation (Nodfor) and the numerical output showing nodal displacement from its original position (Nodout). All the data were

then organized using Excel script taking only necessary information to generate the scatter chart for final analysis.

The final analysis shows that in many origami permutations, the structure lost its stiffness and became similar to a catenary curve, which indicates a buckling within the origami. The catenary is the curve that depicts an idealized hanging chain or cable assumed under its own weight when supported only at its both ends. In general, such sudden structural failure is due to high compressive stress and causes deformation of the whole structure. However, the evaluation also shows that as the angle between the mid-rib and the vein increases, the total Z reactions decrease, indicating that the higher the overall height of the origami is (see Fig. 5), the more stable the structure becomes. The result also shows that as the tessellation density increases to 16x14, less deflection (Z displacement) occurs, which produces a more stable structure because it has more media spread as modules channel the load of gravity to the big kneel truss, which helps to stiffen the structure. For the angle of deployment, the graph of reaction forces shows that at a folding angle of 75% (contracted mode), most of the permutation structurally failed, which indicates the limitation of the deployment of the origami. The result also shows that at the permutation with thicker edges, for instance, the reaction is not as extreme as the other permutation with thinner edges. This is because thicker edges act like a truss, which begins to approximate the application of the origami truss to tessellation. The overall result shows that the permutation with a higher angle between the mid-rib and the vein, higher density and thicker edges are structurally more stable.

8. CONCLUSIONS

The research study the combined method between the utilization of parametric system, geometric scripting and non-linear Finite Element Analysis in order to analyze a deployable structure. The overall study proved to be successful in terms of understanding the geometric and structural behavior of the Miura-ori through a parametric modeling and a non-linear analysis approach. Interoperability from the parametric to the structural analysis system is achieved in that all data of nodal coordinates as well as element construction to materiality are successfully exchangeable. However, the overall data exchange requires a tedious process and proved to be inefficient. The data filtration of Nodfor and Nodout from LS-Dyna requires a purely mathematical process and proved to be successful in terms of data management but still lacks visual interface.

The overall process involved massive amount of scripted works which dealt with the geometric construction and the organization of topological index where overlapped points were strictly restricted. The combination of parametric system and geometric scripting capable of producing permutable geometry that can be integrated with the FE tool. The integration of those methods combined with FE tool capable of representing large scale non-linearities. The explicit finite element method used by LS-DYNA is able to simulate large deformation of a structure and respond to post-buckling activity of a structure. This become important when analyzing structure with dramatic changes in flexural stiffness such as Miura-ori case as the angle of deployment varies ($\alpha = 30^\circ - 80^\circ$). LS-DYNA is proven capable to simulate this overall complex behavior

For future study, the parametric system can be further developed so as to have the capability to generate curved Miura-ori tessellation with deployability. This would require the process to interpret the folding and unfolding mechanism of the origami in a bended mode instead of flattened.

9. REFERENCES

- [1] Baerlecken, D.; Swarts, M.; Gentry, R.; Wonoto, N.: Bio-Origami: Form finding and evaluation of origami structures, eCAADe 2012: The 30th International Conference on Education and Research in Computer Aided Architectural Design in Europe, Czech Technical University, Prague, Czech Republic, 2012.
- [2] Durreisseix, D.: An overview of mechanisms and patterns with origami, International Journal of Space Structures, 27(1), 2012, 1-14.
- [3] Forbes, Wm.: How a beetle folds its wings, Psyche 31, Cornell University, Ithaca, N.Y , 1924, 254-258

- [4] Gerschutz, M.; Haynes, M.; Nixon, D.; Colvin, J.: Tensile strength and impact resistance properties of materials used in prosthetic check sockets, copolymer sockets, and definitive laminated sockets, *Journal of Rehabilitation Research & Development*, 48(8), 2011, 987-1004.
- [5] Haas, F.: Geometry and mechanics of folding in Dermaphtera and Coleoptera, M.Phil. thesis, University of Exeter, UK, 1994.
- [6] Hoberman, C.: Reversibly expandable three dimensional structure, United States Patent No. 4,780,344, 1988
- [7] Kim, I.; Hong, S.; Park, B.; Choi, H.; Lee, J.: Polyphenylene ether/glycol modified polyethylene terephthalate blends and their physical characteristics, *Journal of Macromolecular Science: Physics*, 51(4), 2012, 798-806.
- [8] Kobayashi, H.; Kresling, B.; Vincent, J. F. V.: The geometry of unfolding tree leaves, *Proc R Soc Lond, B* 265, 1997, 147-154.
- [9] Sorguc, A. ; Hagiwara, I. ; Selcuk, S.: Origamics in architecture: A medium of inquiry for design in architecture, *METU Journal of the Faculty of Architecture*, 26(2), 2009, 235-247.
- [10] Tachi, Tomohiro.: Rigid-foldable thick origami. In Wang, Patsy.; Lang, Robert.; Yim, Mark (eds.), *Origami 5*, 2011, CRC press, Taylor & Francis Group, USA, 253-289.
- [11] Wu, Weina.; You, Zhong.: Modelling rigid origami with quaternions and dual quaternions, *Proceedings of the Royal Society A: Mathematical, physical and engineering sciences*, 466(2119), 2010, 2155-2174.